

Monte Carlo simulations of temperature-programmed desorption spectra

A. P. J. Jansen

Schuit Institute of Catalysis, Eindhoven University of Technology, P.O. Box 513, 5600 MB Eindhoven, The Netherlands

(Received 5 August 2003; published 29 January 2004)

We show how to obtain good quantitative data on the energetics of surface reactions by fitting results of dynamic Monte Carlo simulations to results of kinetic experiments. In particular, we can obtain numerical values for various lateral interactions by simulating temperature-programmed desorption spectra and fitting the simulated spectra to the experimental ones using evolution strategies. We illustrate the procedure by determining nearest-, next-nearest-, and next-next-nearest-neighbor interactions for CO on Rh(100).

DOI: 10.1103/PhysRevB.69.035414

PACS number(s): 68.43.Fg, 68.43.Vx, 82.20.Wt

I. INTRODUCTION

Temperature-programmed desorption (TPD) is one of the most widely used techniques in heterogeneous catalysis and surface science.¹ It has been used to show the importance of lateral interactions for the kinetics of surface reactions, but so far it has not been completely successful in obtaining quantitative data for these interactions. One can often get a reasonable fit of an experimental TPD spectrum with a single parameter for the lateral interactions with the rate equation

$$\frac{d\theta}{dt} = -\nu e^{-(E_{\text{act}}^{(0)} - B\theta)/k_{\text{B}}T} \theta^n. \quad (1)$$

Here θ is the coverage, t is time, T is temperature, k_{B} is the Boltzmann constant, $E_{\text{act}}^{(0)}$ is the activation energy for desorption in the absence of lateral interactions, ν is the prefactor for desorption, n is the order of the reaction, and the lateral interactions are modeled with the parameter B . The problem with this form is the interpretation of this parameter. Equation (1) is a purely phenomenological expression. A simple physical model would be that the adsorbates are randomly distributed over the sites and there is no correlation between the occupation of neighboring sites. This mean-field approximation leads to

$$\frac{d\theta}{dt} = -\nu e^{-E_{\text{act}}^{(0)}/k_{\text{B}}T} \theta [1 + \theta(e^{\phi_{\text{NN}}/k_{\text{B}}T} - 1)]^Z \quad (2)$$

for simple desorption of an atom or molecule that has an interaction ϕ_{NN} with each of its Z nearest neighbors. If the interaction is small, then Eq. (1) is a good approximation of Eq. (2) with $B = Z\phi_{\text{NN}}$. An advantage of this model is that it can easily be extended to more complicated reactions and to models with more lateral interaction parameters. It has been used successfully to explain oscillations in NO hydrogenations.^{2,3} A weak point of the model is that the absence of correlation in the occupation of sites is contradictory to the presence of lateral interactions. Even at high temperatures when there is no long-range order, there is still short-range order (i.e., correlation), and Eq. (2) does not hold.

Correlation can be included by using pair approximations, such as the quasichemical approximation or even more sophisticated approximations.⁴⁻⁶ Although these approxima-

tions clearly improve on mean field, they are still approximations. Density-functional theory (DFT) calculations for a number of systems have shown that there are generally more than one interaction of appreciable magnitude between adsorbates.⁷⁻¹⁰ Analyses of the heat of adsorption as a function of coverage,¹¹ phase diagrams of adlayers,^{12,13} and other experiments point to the same fact. These lateral interactions can differ substantially and, as will be shown, can determine different properties of a system. It is not clear then that the approximations mentioned above are always reliable.

An accurate description of the kinetics of surface reactions with lateral interactions can be given by dynamic, or kinetic, Monte Carlo (DMC) simulations.¹⁴⁻¹⁹ We will show in this paper that it is possible to determine numerical values for various substantially different lateral interaction parameters with DMC simulations of TPD. This is obvious of great benefit. If lateral interactions can be obtained from such a widely used technique as TPD, it may be possible to obtain a large amount of quantitative data on these interactions for many systems. Apart from the lateral interactions our method also yields the activation energy and prefactor for desorption. It also gives error estimates that indicate how relevant a specific lateral interaction is for the kinetics. We will illustrate the method on CO desorption from Rh(100).²⁰ We will determine lateral interactions between nearest, next-nearest, and next-next nearest neighbors. There is a strong repulsion between neighboring sites. This repulsion leads to an ordered $c(2 \times 2)$ structure of the adlayer even at the temperatures where desorption takes place, but it hardly affects the spectra, which are determined by the next- and next-next-nearest-neighbor interactions.

II. COMPUTATIONAL DETAILS

A. The model for CO/Rh(100)

CO adsorbs onto top sites of Rh(100) for the coverages below $\theta = 0.5$ that we will look at.²⁰ This means that we use a square grid for the adsorption sites. For the fit of the TPD spectra a grid size of 256×256 was used. There are two processes; CO can desorb or it can diffuse by hopping to a neighboring site if that site is vacant. For both processes we write the rate constant k as^{17,18}

$$k = \nu e^{-E_{\text{act}}/k_{\text{B}}T}. \quad (3)$$

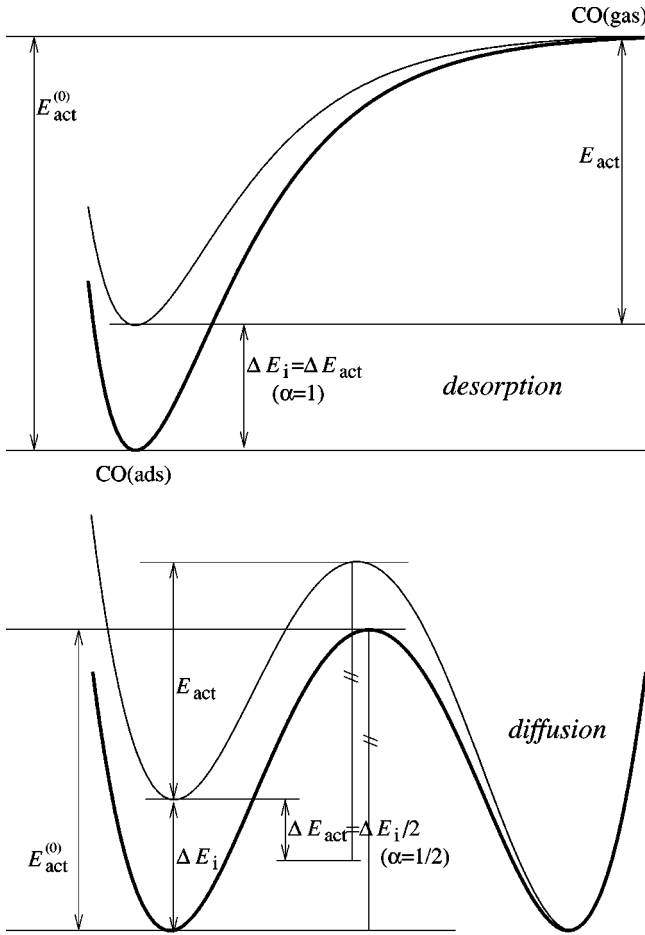


FIG. 1. Energy profiles for desorption and diffusion. The sketches indicate how the activation energies are affected by the lateral interactions. The thick curves show the situations without lateral interactions. The thin curves show the situations with lateral interactions. (For simplicity a situation is shown for diffusion in which only one side of the profile is changed.) For desorption we have a late barrier and a Brønsted-Polanyi parameter $\alpha=1$. For diffusion we have an intermediate barrier with $\alpha=1/2$.

The activation energy is written as $E_{\text{act}} = E_{\text{act}}^{(0)} + \Delta E_{\text{act}}$, where $E_{\text{act}}^{(0)}$ is the activation energy without lateral interactions and ΔE_{act} is the change due to lateral interactions. We assume a Brønsted-Polanyi relation $\Delta E_{\text{act}} = \alpha[\Delta E_f - \Delta E_i]$, with ΔE_f (ΔE_i) the effect of the lateral interactions on the adsorption energy of CO after (before) the reaction has taken place.²¹ For desorption we have assumed a late barrier; $\alpha=1$ (see Fig. 1). Because there are no lateral interactions in the gas phase we have $\Delta E_f=0$. We have assumed that the lateral interactions are pairwise additive so that $\Delta E_i = \sum_{kl} \delta_k \delta_l \phi_{kl}$, with the summation k over all sites involved in the reaction (just one for desorption), the summation l over all surrounding sites (12 sites for desorption), ϕ_{kl} the lateral interaction between adsorbates at sites k and l , and δ_k and δ_l equal to 1 if the site is occupied and 0 otherwise. We have included nearest-neighbor ϕ_{NN} , next-nearest-neighbor ϕ_{NNN} , and next-next-nearest-neighbor interactions ϕ_{NNNN} (see Fig. 2). Positive values indicate repulsion and negative ones attraction.

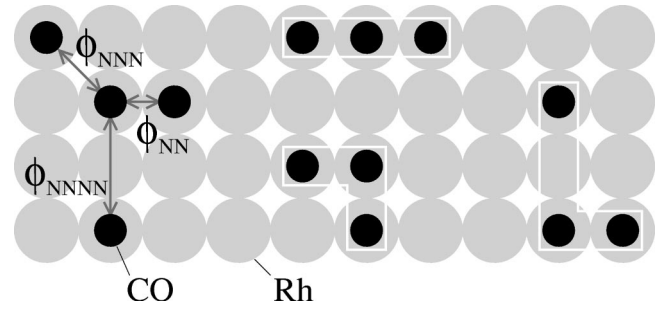


FIG. 2. Definition of the pairwise interactions ϕ_{NN} , ϕ_{NNN} , and ϕ_{NNNN} on the left. The three-particle interactions in the middle are neglected; these configuration do not occur because ϕ_{NN} is large and positive. The three-particle interaction, and similar ones, on the right are neglected because they are small.

We expect three-particle interactions with at most one pair of CO molecules at nearest-neighbor sites to be negligible (see Fig. 2). Three-particle interactions with two pairs of CO molecules being nearest neighbors may be of a similar magnitude as weak pair interactions.⁷ However, the nearest-neighbor pair interactions ϕ_{NN} will be shown to be so large that such configurations are very unlikely. Therefore we have neglected all three- and more-particle interactions. We have also assumed that the prefactors are not affected by the lateral interactions. This agrees with what has been found for similar systems: CO on Ni(100), Cu(100), and Pd(100) at low coverages.²² CO also adsorbs at bridge position when the coverage is above 0.5 ML (monolayer).²⁰ This is a much more complicated situation, because the number of kinetic parameters is more than double the number of kinetic parameters for low coverages. Therefore we have only looked at coverage $\theta \leq 0.5$.

Diffusion of CO is very fast. If realistic diffusion rates will be used, almost all computer time would be spent on the diffusion. Fortunately, the rate constant for diffusion can be reduced drastically without affecting the results of a simulation. The reason for this is that the main role of diffusion is to equilibrate the adlayer. This can be accomplished with a reduced diffusion as follows (see also Fig. 3). The effect of lateral interactions on the activation energy for diffusion is given by the same expressions as for the activation energy for desorption. Differences are that we have an intermediate barrier, $\alpha=1/2$, $\Delta E_f \neq 0$ but is given by $\Delta E_f = \sum_{kl} \delta_k \delta_l \phi_{kl}$, and there are more sites involved. (The summation over k is over two sites and the one over l is over 16 sites.) The activation energy $E_{\text{act}}^{(0)}$ for diffusion was chosen as the minimal value that gives $E_{\text{act}} = E_{\text{act}}^{(0)} + \Delta E_{\text{act}} \geq 0$ for all possible configurations of the CO molecules. The value was determined for each simulation separately. By taking a minimal value for $E_{\text{act}}^{(0)}$ the variation of the diffusion rate as a function of temperature was minimized. Note that changing $E_{\text{act}}^{(0)}$ does not change the equilibrium of the adlayer in any way (see Fig. 3). This depends only on ΔE_{act} , and the way that ΔE_{act} is affected by the lateral interactions (see above) ensures that the different adlayer configurations occur with a proper probability given by a Boltzmann factor. The prefactor for diffusion was also given a minimal value, but large enough so that

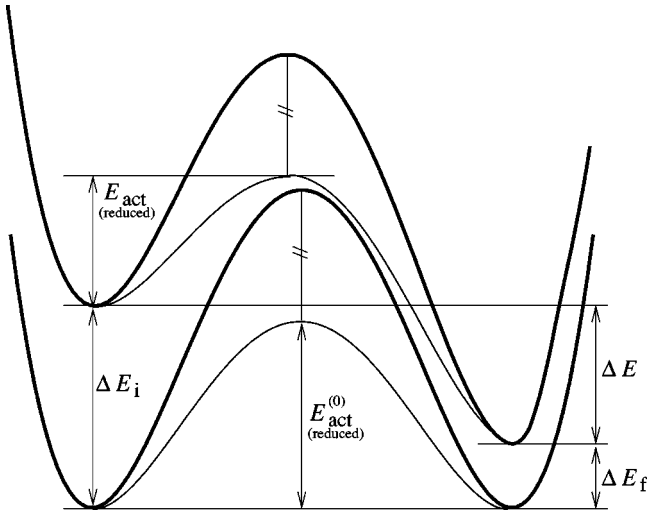


FIG. 3. Energy profile for diffusion and how it changes when we reduce activation energy in the absence of lateral interactions. The equilibrium of the adlayer depends on the energy differences $\Delta E = \Delta E_f - \Delta E_i$, but not on the height of the activation barrier. The activation energy $E_{\text{act}}^{(0)}$ affects only this height.

the adlayer was equilibrated at all times. This value of the prefactor was determined experimentally by varying it and determining the range for which the results did not change. Together with the way that the activation energy is chosen, this ensures that a minimal fraction of the simulation time is spent on the diffusion.

B. Dynamic Monte Carlo

We have used DMC to simulate the evolution of the adlayer using the CARLOS code.²³ Our method can be derived from first principles, and gives exact results for the model that we use for CO on Rh(100).^{17,18} There are numerous DMC algorithms that can be used, which all give statistically exactly the same results.^{16,24,18} All DMC algorithms generate an ordered list of times at which a reaction takes place, and for each time in that list the reaction that occurs at that time. A DMC simulation starts with some chosen initial configuration. The list is traversed and changes are made to the configuration corresponding to the occurring reactions. The various algorithms differ in how the reaction times are computed, how a reaction of a particular type is chosen, and how it is determined where on the surface a reaction takes place. We have used the first-reaction method in all our simulations, because this method gives exact results also when the rate constants vary in time as in a TPD experiment.^{15,16,18,24,25}

C. Evolution strategies

The simulated spectra can be very noisy because we are using stochastic simulations. The noise can be reduced but only at the cost of an increase in computer time. The noise scales as $O(L^{-1})$, with L the linear dimension of the grid, and the computer time for simulating a TPD spectrum scales as $O(L^2 \ln L)$ with the first-reaction method.¹⁶ The method that we have chosen to fit the simulated spectra to the experimental ones is evolution strategy (ES).^{26,27} This method

is able to deal with noisy data. In addition, it is a method that does not get trapped in the first local optimum that is encountered. It is a method from the field of evolutionary computation.²⁷ It shares many characteristics with the better known method genetic algorithms,²⁸ but ES seems better suited to optimize sets of real numbers.²⁷ (We also tried Powell's method and simulated annealing to fit the experimental spectra.²⁹ Powell's method managed to converge in spite of the noise, but generally gave bad fits, because it got trapped in the nearest local minimum. Simulated annealing gave fits of the same quality as ES, but seemed to be somewhat less efficient.)

For each set of kinetic parameters (prefactor, activation energy, and lateral interactions) we computed $\chi^2 = \sum_{i=1}^{N_{\text{exp}}} \chi_i^2 / s_i^2$, where i stands for TPD spectra with different initial coverage, N_{exp} is the number of such spectra, s_i is an error estimate, and χ_i^2 is the difference between the experimental and the simulated spectrum defined as

$$\chi_i^2 = \frac{1}{N_{\text{sample}}} \sum_{j=1}^{N_{\text{sample}}} [r_{ij}^{(\text{exp})} - r_{ij}^{(\text{sim})}]^2, \quad (4)$$

where $r^{(\text{exp})}$ and $r^{(\text{sim})}$ stand for desorption rates in the experiment and the simulation, respectively. The sum is over different temperatures $T_0 + j\Delta T$. The error estimates s_i were determined by assuming that the errors are mainly due to the numerical noise in the simulations. We did 101 simulations with the same initial conditions and kinetic parameters. For each subsequent pair of simulations we calculated χ_i^2 , and for s_i^2 we took the average of $\chi_i^2/2$ over the 100 pairs. (There is a factor 1/2, because we are calculating χ_i^2 from two simulations, whereas in the fit there is only one simulation.) We looked at $N_{\text{exp}}=8$ different initial coverages, and we used $T_0=250$ K, $N_{\text{sample}}=401$, with $\Delta T=1$ K, and a heating rate of 5 K/sec.

The ES that we have used works with a set of pairs $(\mathbf{x}_i, \boldsymbol{\sigma}_i)$, with $i=1, 2, \dots, \mu$, where \mathbf{x}_i and $\boldsymbol{\sigma}_i$ are vectors of real numbers and μ is the number of pairs. The set is called a population and the pairs can be considered genetic material. The components of the vector \mathbf{x} are the kinetic parameters that we want to determine. To minimize χ^2 we generate a new population, which we hope contains better kinetic parameters than the original one. We generate a new population by first generating λ offspring by randomly choosing two pairs $(\mathbf{x}_k, \boldsymbol{\sigma}_k)$ and $(\mathbf{x}_l, \boldsymbol{\sigma}_l)$ and making a so-called intermediate crossover $[(\mathbf{x}_k + \mathbf{x}_l)/2, (\boldsymbol{\sigma}_k + \boldsymbol{\sigma}_l)/2]$. Then we mutate each of the λ offspring as follows: $x_\alpha \rightarrow x_\alpha + N(\sigma_\alpha)$ and $\sigma_\alpha \rightarrow \sigma_\alpha \cdot \exp[N(\Delta\sigma)]$, where α indicates a component of the vector and N is a random number drawn from a Gaussian distribution centered at the origin and a width given by the argument. The quantity $\Delta\sigma$ is a parameter of the method. Finally for each of the λ offspring we compute χ^2 by doing a set of DMC simulations. The new population will then consist of the μ pairs from the λ offspring with the lowest χ^2 (comma selection). We have typically generated 50 populations during a single run with $\mu=32$, $\lambda=64$, and $\Delta\sigma=0.5$. A single run consisted of about 25 000 DMC simulations. This took at most only a little over 2 days on a 600 Mhz Pentium III PC.

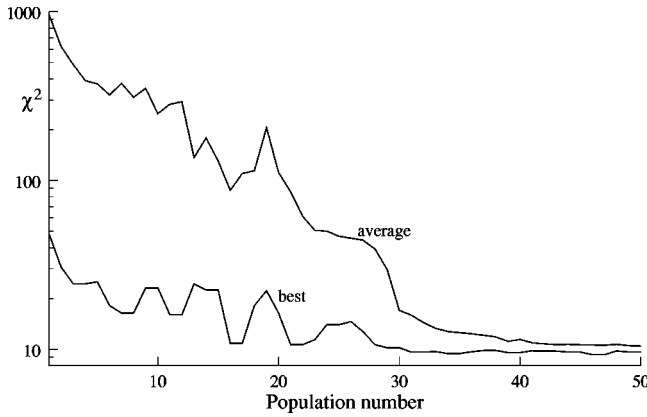


FIG. 4. Convergence of the evolutionary computation. The lines show the error estimate χ^2 for the best set of kinetic parameters for CO desorption from Rh(100) in the subsequent populations and the average of all sets in each population.

III. RESULTS AND DISCUSSION

There are two kinds of errors when we fit the experimental spectra. We have errors because our DMC is a stochastic method and we may have errors because our model of the lateral interactions may be deficient. The total error is an unknown combination of the errors of both types. We are mainly interested in possible shortcomings of our model of the lateral interactions. To get an idea of the errors caused by the DMC simulations we have done some preliminary fits to obtain lateral interactions. The best preliminary fit was obtained with $\phi_{\text{NN}} \approx 25$ kJ/mol, $\phi_{\text{NNN}} \approx 1.3$ kJ/mol, and $\phi_{\text{NNNN}} \approx 1.0$ kJ/mol with the prefactor and the activation energy fixed at experimental values of $\nu_{\text{des}} = 6.31 \times 10^{13} \text{ sec}^{-1}$ and $E_{\text{act}}^{(0)} = 137$ kJ/mol.²⁰ We then generated TPD spectra with these parameters using DMC and a grid of size 1024×1024 to minimize the noise of the simulations. We then tried to fit these simulated spectra in exactly the same way as we fitted the experimental spectra. Because the simulated spectra could, in principle, be fitted exactly, the errors were due only to the stochastic nature of the DMC simulations. The best fit to the simulated spectra was found to be $\nu_{\text{des}} = 9.28 \times 10^{13} \text{ sec}^{-1}$, $E_{\text{act}}^{(0)} = 139$ kJ/mol, $\phi_{\text{NN}} = 17$ kJ/mol, $\phi_{\text{NNN}} = 1.4$ kJ/mol, and $\phi_{\text{NNNN}} = 1.0$ kJ/mol with $\chi^2 = 3.9$. We see that the fit is reasonable for the prefactor and the activation energy, bad for ϕ_{NN} , and excellent for ϕ_{NNN} and ϕ_{NNNN} . We will show below why this is the case. More important here is the value of χ^2 . If the fit of the experimental spectra gives a much higher value, then this would point to shortcomings of our model for the lateral interactions.

Figure 4 shows a typical result for the convergence of the determination of the lateral interactions and other kinetic parameters for CO desorption from a Rh(100) surface using ES. Note that the overall trend is that the best set of parameters in and the average of each population improves, but quite often a new population may also be worse than the previous one. This indicates the ability of ES to search for a global minimum.

Figure 5 shows the experimental and simulated TPD spectra with the kinetic parameters that give the best fit.²⁰ We see

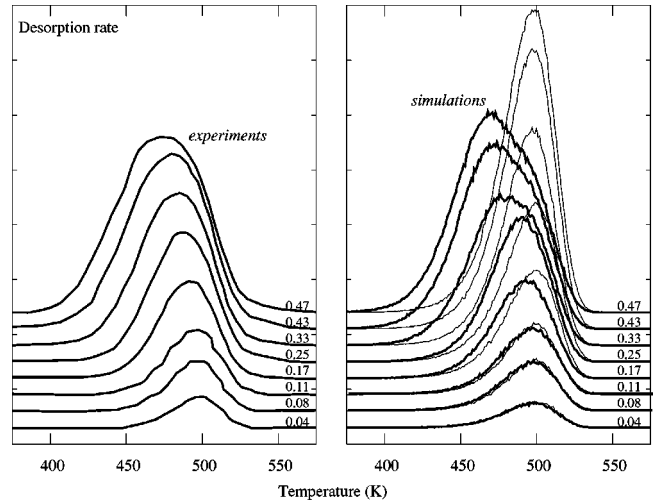


FIG. 5. Experimental (left) and simulated (right) temperature-programmed desorption spectra for CO/Rh(100). Each simulated spectrum was obtained from a single simulation with a grid of 1024×1024 points. The values on the right of each set of curves indicate initial coverages. The curves are offset vertically to make them easier to distinguish. The thin curves on the right are simulated spectra with the lateral interactions switched off. The heating rate is 5 K/sec.

that the agreement is very good. Our best set of kinetic parameters is $\nu_{\text{des}} = 1.435 \times 10^{12} \text{ sec}^{-1}$, $E_{\text{act}}^{(0)} = 121$ kJ/mol, $\phi_{\text{NN}} = 24$ kJ/mol, $\phi_{\text{NNN}} = 1.1$ kJ/mol, and $\phi_{\text{NNNN}} = 0.9$ kJ/mol with $\chi^2 = 9.3$, which should be compared to 3.9, which is the value that is obtained by trying to fit simulated spectra (see above). We note that, as χ^2 is a quadratic form, the error is only about 50% larger, because of shortcomings of our model and experimental errors. This means that the model for the lateral interactions is acceptable.

The procedure does not always converge to exactly the same minimum. In fact, we can get an even better fit than the one mentioned above for small values of ϕ_{NN} . For example, $\nu_{\text{des}} = 6.31 \times 10^{13} \text{ sec}^{-1}$, $E_{\text{act}}^{(0)} = 137$ kJ/mol, $\phi_{\text{NN}} = 2.4$ kJ/mol, $\phi_{\text{NNN}} = 1.3$ kJ/mol, and $\phi_{\text{NNNN}} = 1.5$ kJ/mol gives $\chi^2 = 8.7$. The drawback of this set is that it allows adlayer structures at low temperature that are not found experimentally. Up to coverages of 0.5 ML a $c(2 \times 2)$ structure is found.²⁰ This points to strong repulsion between CO molecules at nearest-neighbor sites. The set above with small ϕ_{NN} yields a $(\sqrt{2} \times \sqrt{2})$ - 2O structure at low temperature. The set of kinetic parameters with high ϕ_{NN} value was obtained with constraints that made the $c(2 \times 2)$ structure more stable than a number of other possible structures. Such constraints can easily be included in ES.

If the next-next-nearest-neighbor interaction is neglected, then the fit becomes a bit less good with $\chi^2 = 11.2$ and $\nu_{\text{des}} = 2.04 \times 10^{12} \text{ sec}^{-1}$, $E_{\text{act}}^{(0)} = 123$ kJ/mol, $\phi_{\text{NN}} = 13$ kJ/mol, and $\phi_{\text{NNN}} = 2.0$ kJ/mol. Note that the prefactor and the activation energy for an isolated molecule is almost the same as for the best fit. The nearest-neighbor interaction is quite different for reasons that we will discuss below. The next-nearest-neighbor interaction is about equal to the sum of ϕ_{NNN} and ϕ_{NNNN} of the best fit. This is an indication that this

is an important quantity determining the spectra.

We have repeated the fit a number of times, looked at the statistics of the results, and derived estimates for the accuracy of the kinetic parameters. The results of this procedure are $\ln(\nu_{\text{des}}/\text{sec}^{-1}) = 12.2_{-0.2}^{+0.7}$, $E_{\text{act}}^{(0)} = 121_{-1}^{+7}$ kJ/mol, $\phi_{\text{NN}} = 24_{-3}^{+8}$ kJ/mol, $\phi_{\text{NNN}} = 1.1_{-0.2}^{+0.4}$ kJ/mol, and $\phi_{\text{NNNN}} = 0.9_{-0.3}^{+0.3}$ kJ/mol. These are best values with one-sided standard deviations. We see that the errors for the prefactor ν_{des} and the activation energy $E_{\text{act}}^{(0)}$ are quite substantial. The main cause for this is a compensation effect; a TPD spectrum changes very little when the activation energy and the prefactor are decreased or increased simultaneously.³⁰ Experimental values are found in the range $\ln(\nu_{\text{des}}/\text{sec}^{-1}) = 12.9\text{--}16.3$ and $E_{\text{act}}^{(0)} = 134\text{--}149$ kJ/mol.²⁰ The most recent values are $\nu_{\text{des}} = 10^{13.8 \pm 0.2} \text{sec}^{-1}$ and $E_{\text{act}}^{(0)} = 137 \pm 2$ kJ/mol in the low coverage limit. The agreement with our result is reasonable. In fact, the desorption rate constant for an isolated molecule is the same for the experimental values and the best-fit values at $T = 500$ K, which is the peak maximum temperature at low coverage (see Fig. 5). Measurements of the heat of adsorption gave a value of 118 ± 4 kJ/mol, which is also in good agreement with our best-fit values if we assume that CO adsorption is not or only weakly activated.¹¹

The large error in ϕ_{NN} is due to the weak dependence of the TPD spectra on this lateral interaction. The value of ϕ_{NN} is large and the CO molecules will avoid occupying neighboring sites. This lateral interaction only affects how easy it is for the adlayer to rearrange itself when CO molecules start desorbing, but when a CO molecule desorbs it rarely has a nearest neighbor, so there is no direct effect on the TPD spectra. This means that one cannot really determine the value of ϕ_{NN} from TPD. Although the interaction between nearest neighbors need not be known precisely, one should not prevent CO molecules occupying nearest-neighbor position altogether. For $\phi_{\text{NN}} \rightarrow \infty$ we find a best fit with $\chi^2 = 11.3$. This is clearly higher than our best fit, although not much. Apparently the adlayer wants to move the CO molecules apart. This is easier when there is a small probability that the CO can become nearest neighbors.

The errors in the other lateral interactions are much smaller, because they do affect the TPD spectra substantially. This differs from calculating the lateral interactions with DFT. There strong lateral interactions can be determined quite accurately, but the weak lateral interactions have much larger relative errors.⁹ Coverage-dependent measurements of the heat of adsorption gave $\phi_{\text{NN}} = 9 \pm 1$ kJ/mol, $\phi_{\text{NNN}} = 1.0 \pm 0.5$ kJ/mol, and $\phi_{\text{NNNN}} = -1.0 \pm 0.5$ kJ/mol.¹¹ The nearest-neighbor interaction differs substantially for reasons

mentioned above. The next-nearest-neighbor interaction is in excellent agreement, but the next-next-nearest-neighbor interaction has a different sign. Attractive interactions between adsorbates at next-next-nearest-neighbor positions have been used to explain island formation.³¹ However, if ϕ_{NNNN} is negative, then ϕ_{NNN} should probably be larger, as their sum was found to be very sensitive to the shift of the peaks in the TPD spectra. As there are no details in Ref. 11 on how the lateral interactions are obtained, we cannot properly comment on the origin of the difference between our results and those of that study.

IV. SUMMARY

We have shown that temperature-programmed desorption spectra contain information on the lateral interactions in a system. This information can be extracted and numerical values for lateral interactions can be obtained from these spectra by accurately modeling the surface processes using dynamic, or kinetic, Monte Carlo simulations. Because these simulations are stochastic and the simulated spectra are therefore noisy, we have used evolution strategies to fit the simulated spectra to the experimental ones. We have illustrated the procedure with CO desorption from Rh(100). We have obtained the prefactor and the activation energy for the desorption and the nearest-, next-nearest-, and next-next-nearest-neighbor interactions. The TPD spectra show that the nearest-neighbor interaction is strongly repulsive. It leads to the $c(2 \times 2)$ structure for coverages below 0.5 ML even at the temperature where desorption takes place, but it has only a small effect of the TPD spectra. This also means that the numerical value for the nearest-neighbor interaction can only be determined with a large error. The TPD spectra depend much more on the next- and next-next-nearest-neighbor interactions. These are much smaller, but can also be determined much more accurately. Numerical values for the lateral interactions are $\phi_{\text{NN}} = 24$ kJ/mol, $\phi_{\text{NNN}} = 1.1$ kJ/mol, and $\phi_{\text{NNNN}} = 0.9$ kJ/mol with $\nu_{\text{des}} = 1.435 \times 10^{12} \text{sec}^{-1}$, $E_{\text{act}}^{(0)} = 121$ kJ/mol, for the prefactor and the activation energy for desorption of an isolated CO molecule. Because of the prevalence of TPD, the procedure introduced in this paper will enable us to obtain accurate numerical values for lateral interaction for many adsorbates on many substrates.

ACKNOWLEDGMENT

This work was supported by the National Research School Combination Catalysis (NRSC-C).

¹J.W. Niemantsverdriet, *Spectroscopy in Catalysis* (Wiley-VCH, Weinheim, 2000).

²A.G. Makeev, M.M. Slinko, N.M.H. Janssen, P.D. Cobden, and B.E. Nieuwenhuys, *J. Chem. Phys.* **105**, 7210 (1996).

³A.G. Makeev, N.M.H. Janssen, P.D. Cobden, M.M. Slinko, and B.E. Nieuwenhuys, *J. Chem. Phys.* **107**, 965 (1997).

⁴V.P. Zhdanov, *Elementary Physicochemical Processes on Solid Surfaces* (Plenum, London, 1991).

⁵S.H. Payne and H.J. Kreuzer, *Surf. Sci.* **399**, 135 (1998).

⁶W. Widdra, P. Trischberger, W. Frieß, D. Menzel, S.H. Payne, and H.J. Kreuzer, *Phys. Rev. B* **57**, 4111 (1998).

⁷C. Stampfl, H.J. Kreuzer, S.H. Payne, H. Pfnür, and M. Scheffler,

- Phys. Rev. Lett. **83**, 2993 (1999).
- ⁸E. Hansen and M. Neurock, Surf. Sci. **441**, 410 (1999).
- ⁹A.P.J. Jansen and W.K. Offermans, J. Comput. Meth. Sci. Eng. **2**, 351 (2002).
- ¹⁰C.G.M. Hermse, F. Frechard, A.P. van Bavel, J.J. Lukkien, J.W. Niemantsverdriet, R.A. van Santen, and A.P.J. Jansen, J. Chem. Phys. **118**, 7081 (2003).
- ¹¹R. Kose, W.A. Brown, and D.A. King, J. Phys. Chem. **103**, 8722 (1999).
- ¹²P. Piercy, K. De' Bell, and H. Pfnür, Phys. Rev. B **45**, 1869 (1992).
- ¹³C. Schwennicke and H. Pfnür, Phys. Rev. B **56**, 10 558 (1997).
- ¹⁴K.A. Fichthorn and W.H. Weinberg, J. Chem. Phys. **95**, 1090 (1991).
- ¹⁵A.P.J. Jansen, Comput. Phys. Commun. **86**, 1 (1995).
- ¹⁶J.J. Lukkien, J.P.L. Segers, P.A.J. Hilbers, R.J. Gelten, and A.P.J. Jansen, Phys. Rev. E **58**, 2598 (1998).
- ¹⁷R.J. Gelten, R.A. van Santen, and A.P.J. Jansen, in *Molecular Dynamics: From Classical to Quantum Methods*, edited by P.B. Balbuena and J.M. Seminario (Elsevier, Amsterdam, 1999), pp. 737–784.
- ¹⁸A.P.J. Jansen, <http://arXiv.org/>, paperno. cond-mat/0303028.
- ¹⁹J.S. Reese, S. Raimondeau, and D.G. Vlachos, J. Comput. Phys. **173**, 302 (2001).
- ²⁰A.P. van Bavel, M.J.P. Hopstaken, D. Curulla, J.J. Lukkien, P.A.J. Hilbers, and J.W. Niemantsverdriet, J. Chem. Phys. **119**, 524 (2003).
- ²¹G. Ertl, H. Knoezinger, and J. Weitkamp, *Handbook of Heterogeneous Catalysis* (VCH, Weinheim, 1997).
- ²²V.P. Zhdanov, Surf. Sci. Rep. **12**, 183 (1991).
- ²³CARLOS is a general-purpose program, written in C by J. J. Lukkien, for simulating reactions on surfaces that can be represented by regular grids; an implementation of the first-reaction method, the variable stepsize method, and the random selection method, <http://www.wpa.win.tue.nl/johanl/carlos/>
- ²⁴J.P.L. Segers, Ph.D. thesis, Eindhoven University of Technology, 1999.
- ²⁵D.T. Gillespie, J. Comput. Phys. **22**, 403 (1976).
- ²⁶H.-P. Schwefel, *Evolution and Optimum Seeking* (Wiley, Chichester, UK, 1995).
- ²⁷Z. Michalewicz, *Genetic Algorithms + Data Structures = Evolution Programs* (Springer, Berlin, 1999).
- ²⁸D.A. Goldberg, *Genetic Algorithms in Search, Optimization, and Machine Learning* (Addison-Wesley, Reading, MA, 1989).
- ²⁹W.H. Press, B.P. Flannery, S.A. Teukolsky, and W.T. Vetterling, *Numerical Recipes. The Art of Scientific Computing* (Cambridge University Press, Cambridge, 1989).
- ³⁰R.A. van Santen and J.W. Niemantsverdriet, *Chemical Kinetics and Catalysis* (Plenum, New York, 1995).
- ³¹V.P. Zhdanov and B. Kasemo, Surf. Sci. **415**, 403 (1998).